PAPER • OPEN ACCESS

Influence of moisture content, temperature and absorbed solar radiation on the thermal performance of a spruce XLAM wall in the Italian climates

View the article online for updates and enhancements.

Influence of moisture content, temperature and absorbed solar radiation on the thermal performance of a spruce XLAM wall in the Italian climates

M Danovska[1], G Pernigotto[1], M Baratieri[1], P Baggio[2], A Gasparella[1]

[1] Free University of Bolzano-Bozen, Bolzano, Italy.
[2] University of Trento, Trento, Italy.
Corresponding author e-mail: maja.danovska@natec.unibz.it

Abstract. In building simulation codes, conduction transfer functions or finite difference methods are generally implemented to model the heat transmitted through the opaque components. Thermal conductivity is conventionally assumed constantly equal to its nominal value, even if it depends on both temperature and moisture content, especially for porous building materials, like timber. Therefore, the adoption of constant nominal values can bring inaccuracies on the calculated heat flux, affecting the predicted building energy performance. In this research, the magnitude of such inaccuracies is quantified for a spruce cross-lam (i.e. XLAM) wall, by comparing hourly specific heat fluxes calculated with variable thermal conductivity and those with nominal one. To achieve such a goal, a MATLAB® 1D heat and mass transfer model was developed according to the finite difference method. Material´s thermal conductivity was characterised as a function of moisture content and temperature. Finally, the developed model was calibrated and validated against experimental data collected in the Building Physics Laboratory of the Free University of Bozen-Bolzano. Annual simulations were run considering 110 Italian climates and different orientations and inclinations of the wall. Constant internal boundary conditions and hourly variable external conditions were adopted; in particular, external solicitations were expressed through the sol-air temperature definition.

1. Introduction

Wood is playing an important role in the building sector because of its low environmental impact and its quite good insulating properties [1, 2]. This allows for a lowering of the energy consumption of buildings, 41 % of final energy uses in Europe, more than 60 % of which is due to space heating [3]. However, in porous materials like wood, the thermal performance is strongly affected by the temperature and the moisture content. Usually, materials´ thermal conductivity is measured in reference conditions set by EN ISO 10456 [4] but when a material is placed in operation in the envelope it is subjected to different moisture and temperature conditions. Measured deviations of nominal thermal conductivity in wood can reach 35 % at higher temperatures [6]. In the same way, some studies [5-10] observed that thermal conductivity of a moist material can be from 12 % to 61 % higher than in dry conditions depending on the mean specimen's temperature. This is clearly due to water thermal conductivity, which is 25 times higher than the air. This temperature-moisture dependence may affect some building simulation codes (e.g., EnergyPlus and TRNSYS), which usually use constant thermal properties for calculating the heat transfer across a wall and the energy performance of buildings [5]. Hence, this work aims at characterising the thermal conductivity as a function of temperature and moisture content for an improvement in the accuracy of building performance simulation. Further, it investigates the extent to

which the variability of the thermal conductivity influences the heat transfer through a spruce XLAM wall in the Italian climates. The impact of temperature and humidity on thermal conductivity is first investigated experimentally and then a MATLAB® 1D heat and mass transfer model is developed. Annual simulations are run for 110 climates and specific hourly heat fluxes compared to those calculated with nominal thermal conductivity. Constant internal boundary conditions and hourly variable external conditions are adopted. In particular, external solicitations are expressed through the sol-air temperature definition.

2. Methodology

2.1. Experimental activity

The experimental activity aimed at obtaining a correlation between thermal conductivity and materials' temperature and water vapor partial pressure by means of thermal conductivity measurements conducted on 4 spruce specimens of 0.2 x 0.2 x 0.05 m (figure 1) at different temperature and moisture contents in the Building Physics Lab of the Free University of Bozen-Bolzano. Measurements were performed with the calibrated Netzsch HFM 436/3 Lambda™ according to ISO 8301, EN 12664:2001 and EN 12667.

Figure 1. The four analysed spruce specimens

The analysed specimens were equipped with a polystyrene frame to reach the required instrument dimensions and to grant a mono-dimensional heat flux through the measurement section. Temperature was varied from 10 °C to 50 °C in steps of 5 °C and each measurement performed after the instrument had reached thermal equilibrium (i.e., constant heat flux). To study the effect of moisture content on materials thermal conductivity, specimens were conditioned in an ATT Angelantoni DM340 climatic chamber with two different values of relative humidity and equal temperature [4]. Specimens were subjected to a first cycle of humidification and dehumidification [11] and, then, to a drying process at 105 °C [12]. The conditioning process lasted until equilibrium was achieved, i.e., when specimens' weight variation - measured with an electronic balance of precision 0.1 g, was less than 0.1 % compared to the day before. The equilibrium moisture content EMC (%) was evaluated on a dry basis and according to Equation (1), where m_{eq} (kg) is the weight reached by the sample at the equilibrium in the climatic chamber and m_{dry} (kg) is the weight after the drying procedure at 105 °C.

$$EMC = \frac{m_{eq} - m_{dry}}{m_{dry}} \tag{1}$$

After each phase, specimens were wrapped in a thin plastic film to avoid moisture losses, and then, thermal conductivity was measured. Measurements of thermal conductivity were carried out at three different moisture contents (given on a dry basis):

1. *"As-is"* condition, where specimens have a moisture content of 6.3 %.
2. *Humidified* condition at 23 °C and 80 % of relative humidity (13.2 % moisture content).
3. *Dehumidified* condition at 23 °C and 10 % of relative humidity (3.5 % moisture content).

2.2. Mathematical model

To evaluate the effect of the temperature and the moisture on the specific heat flux through a XLAM wall, a 1D heat and mass transfer dynamic model was developed, considering as heat transfer mechanisms, internal conduction and surface convection according to Fourier and Newton laws, respectively. The only mechanism considered for the mass transfer was Fickian diffusion and the water vapor partial pressure as driving potential as suggested in the literature [13]. The linear storage moisture capacity C_m (kg kg^{-1} Pa^{-1}) used in the mass transfer model was obtained from the experiments conducted

on spruce specimens [14] and it was assumed equal to 0.02 kg kg^{-1} Pa^{-1}. The adopted heat and mass transfer equations are given in Equation (2) and (3).

$$\rho\, c\, \frac{\partial T}{\partial t} - \nabla \cdot (\lambda\, \nabla T) = 0 \qquad (2)$$

$$C_m\, \rho\, \frac{\partial p_v}{\partial t} - \nabla \cdot (\delta_p\, \nabla p_v) = 0 \qquad (3)$$

Where T is the temperature (°C), t the time (s), λ the thermal conductivity (W m^{-1} K^{-1}), ρ the material's density (kg m^{-3}) and p_v the water vapour partial pressure (Pa). The main materials' parameters (thermal conductivity and density) were measured or calculated, while others, like specific heat capacity c (1380 J kg^{-1} K^{-1}) and vapor permeability δ_p (kg m^{-1} s^{-1} Pa^{-1}), were taken from the literature and obtained after the calibration of the mass transfer model against experimental data, respectively.

2.3. Implementation

Five simplified XLAM components were modelled assuming equivalent boundary conditions as in a real building, to simulate 4 vertical walls (South-, East-, North- and West-oriented) and one horizontal roof. Each component, 30 cm thick, was modelled with a spatial discretisation of 2.5 cm (13 nodes). Considering that the temperature and the water vapour partial pressure across the components are time-dependent, a discretisation in time was performed with time-step 1 h. In particular, Equation (2) and (3) were discretized in time and space by using the backward finite difference method and the central difference scheme, respectively. The adopted time-step was chosen in accordance to the hourly-external boundary conditions, i.e. air temperature and water vapour partial pressure. Constant internal boundary conditions (20 °C and 50 % relative humidity) and hourly-variable external conditions from reference years were assumed. In particular:

- The external vapor partial pressure was taken from the CTI typical reference year (https://try.cti2000.it/).
- The sol-air temperature $T_{sol\text{-}air}$ was taken as external solicitation to account for the solar irradiance, as in Equation (4):

$$T_{sol-air} = T_{air} + \frac{I\,\alpha - h_{r,sky}(T_{air} - T_{sky})}{h_2} \qquad (4)$$

where T_{air} is the air temperature (°C), I the incident solar irradiance calculated according to the Perez model (W m^{-2}), T_{sky} is the sky temperature (°C) obtained as a result of the simulation of the EnergyPlus software, $h_{r,sky}$ the linearized heat transfer coefficient for the sky (W m^{-2} K^{-1}) and h_2 the external surface heat transfer coefficient (W m^{-2} K^{-1}). Short-wave absorptance coefficient α (-) was set equal to 0.3 for vertical walls, and 0.6 for the roof, according to the Standard UNI 10375:2011 [15].

Annual simulations were run for 110 different Italian provinces and for the five orientations considering two different expressions of the thermal conductivity:

1. nominal thermal conductivity λ_{nom}, measured at 23 °C on specimens in the "as-is" conditions (6.3 % EMC).
2. variable thermal conductivity $\lambda(T, p_v)$, based on a linear correlation from the experimental activity (equation (5)).

The influence of the variable thermal conductivity on the thermal performance of the XLAM component for each location and orientation was evaluated with the following two indicators:

1. Linear percentage trend deviation between the hourly values of specific heat fluxes calculated at the internal surface node with variable thermal conductivity and those with nominal thermal conductivity λ_{nom}. In particular, the deviation was evaluated by plotting the hourly-computed specific heat fluxes, actual (i.e. with variable thermal conductivity) and nominal, in a scatter plot and evaluating the slope of the distribution with respect to the bisector.
2. Annual specific energy difference (expressed as kilowatt-hour per square meter): the cumulated deviations of the positive thermal losses (i.e., heat flux from the internal towards the external side) and the negative thermal losses (i.e., heat flux from the external towards the internal side), depending on the heat flux direction.

3. Results and discussions

3.1. Experimental investigation

Table 1 shows the equilibrium weight and the equilibrium moisture content (*EMC*) for each conditioning point (temperature and relative humidity) for one of the tested specimens.

Table 1. Weight (g) and moisture content (%) for each conditioning point.

	"As-is"	Humidified	Dehumidified
Weight (g)	692	737	674
Moisture content (%)	6.3	13.2	3.5

The behavior of the other specimens was similar. The measured dry weight was 651.0 g. The humidification lasted 43 days with a mass increase of 6 % with respect the "as-is" condition. The dehumidification lasted, instead, 9 days with a mass loss of 5 %. This difference in conditioning days shows the hysteresis phenomenon in wood. The drying process lasted 3 days with a mass loss of 6 % with respect to the "as-is" condition. The vapor resistance factor resulted from a calibration of the mass transfer model against experimental data. In particular, the vapor resistance factor was adjusted, by comparison with the dehumidification test, by verifying that the simulated mass loss after 9 days of dehumidification was the same of the experimental one (i.e., 34 g) and that simulated and calculated mean water vapor fluxes were corresponding. A value of vapor resistance factor equal to 32 was obtained and checked in the literature. The model was then verified with humidification data. Both specific heat capacity and vapor resistance factor are input of the models' equations. A nominal thermal conductivity λ_{nom} of 0.107 W m^{-1} K^{-1} was obtained in the "as-is" conditions at 23 °C. Figure 2 illustrates thermal conductivity trends as a function of the specimen's temperature for three different moisture conditions, i.e., "as-is", humidified and dehumidified, for one specimen, since others present the same behavior.
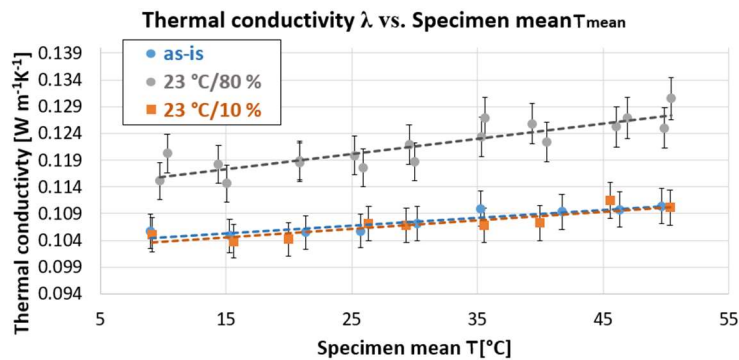

Figure 2. λ vs. mean temperature of a specimen in three different moisture conditions: "as-is" (blue), humidified (grey) and dehumidified (orange), where vertical bars represent the measurement uncertainty (3 %).

Thermal conductivity increases with temperature in all the three cases and the maximum difference obtained in the "as-is" condition (*EMC* equal to 6.3 %) is equal to 11.3 %. With a higher *EMC*, in the humidified condition, the maximum difference obtained at a reference temperature of 23 °C was 13.2 % with respect the "as-is". Dehumidified thermal conductivity (*EMC* equal to 3.5 %) has similar values to those in the "as-is" condition (differences < 3 %). This means that thermal conductivity has a strong non-linear behavior and hysteresis phenomena can be observed associated to humidification and dehumidification cycles. Furthermore, below an *EMC* of at least 6.3 % the effect of moisture on the thermal conductivity is negligible. Equation (5) shows the obtained linear correlation between thermal conductivity (W m^{-1} K^{-1}) and mean specimens' temperature (°C) and water vapor partial pressure (Pa).

$$\lambda(T,p_v)=0.1 + 2.1\cdot 10^{-4}\cdot T + 7.4 \cdot 10^{-6}\cdot p_v \tag{5}$$

3.2. Sol-air temperature trend
Figure 3 shows sol-air temperature profiles for each orientation and for Palermo on the first day of July.
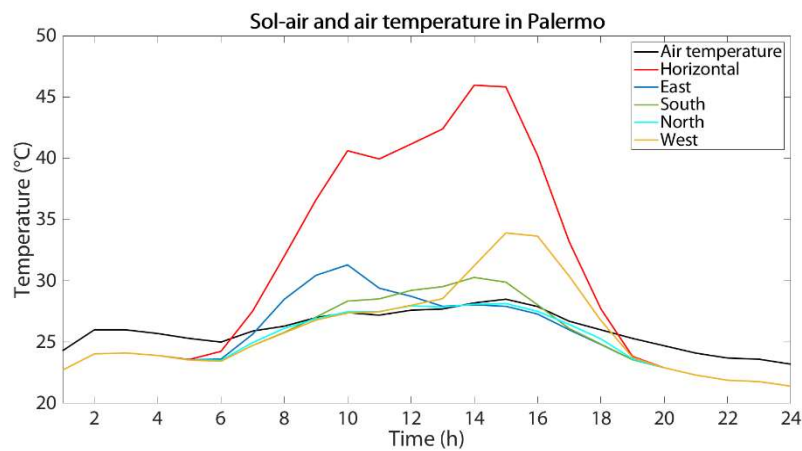

Figure 3. Example of sol-air temperature profiles for July 1st in Palermo, where black, red, blue, green, orange and yellow lines represent air temperature and horizontal, east, south, north and west sol-air temperatures, respectively.

During the day, the horizontal sol-air temperature has an overall profile which is above the other sol-air temperatures (e.g., maximum value is 46 °C around mid-day). East and West temperatures have their maximum peaks between 30 and 35 °C but they are shifted according to the sun path. South sol-air temperature reaches a peak of 30 °C around mid-day. As regards the North-temperature, its profile deviates little from the air temperature and differences are in the order of tenth of a degree because the direct radiation does not hit the northern wall. In the nighttime, sol-air profiles assume the same value because of the absence of radiation and are usually lower than the air temperature because of the infrared losses towards the sky vault.

3.3. Trend of percentage deviations
Figure 4 shows average percentage deviations of the specific heat flux calculated with the variable thermal conductivity with respect the nominal one for each location and just for two orientations (i.e., north and horizontal). Since among vertical walls deviation trends are similar, for sake of simplicity, just the northern wall was represented. The effect of the variable thermal conductivity is to increase the actual heat flux across the components. Deviations range from 1 % to 5 % considering all the orientations. In particular, for the northern wall, the average and the median deviations are 1.7 %, the first quartile 1.2 % and the third quartile is 2.1 %. The minimum value is 0.5 % in Livorno and the maximum is 3 % in Catania, in accordance with the sol-air temperature value, which is usually higher in southern locations than in northern ones (in line with the solar radiation trend). A deviations' distribution along Italy can be noticed: highest values in the South and lowest in the North. This is explained by the magnitude of temperature difference across the wall and the magnitude of the heat flux, as well, which are lower in the south and higher in the north. As regards the roof, deviations are distributed in the same way of the northern one, but values are higher. The average value is 2.8 %, the median 2.7 %, the first quartile 2 % and third quartile 3.4 %. The minimum value is 1.3 % in Aosta and the maximum one of 5 % is again in Catania. Higher percentages are explained by the higher solar radiation on a horizontal surface, especially in summer. Indeed, by looking at the specific heat flux profiles, it can be noticed that, in winter, nominal and actual fluxes are comparable since the effect of the sol-air temperature is moderate, while in summer, the actual heat flux deviates more from the nominal one, and this affects the overall deviation.
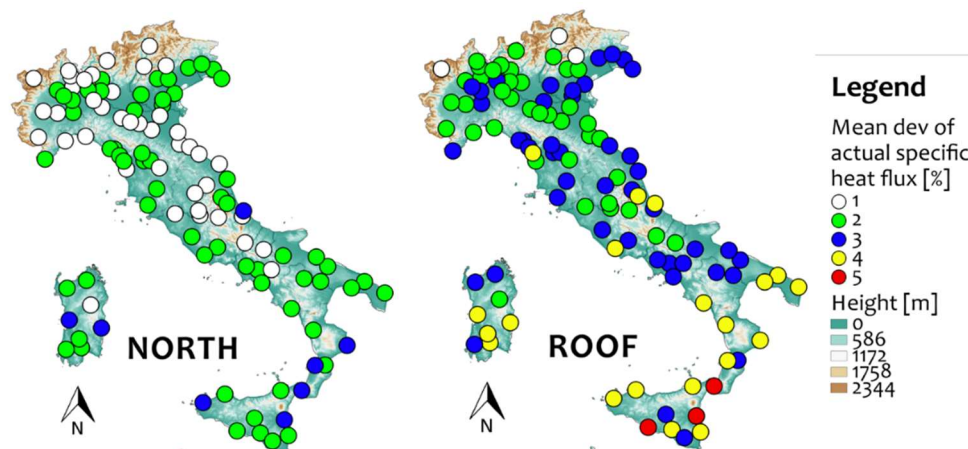
Figure 4. Percentage deviation [%] of the actual heat flux with respect the nominal one for each location in Italy and for the northern and horizontal (roof) orientation.

3.4. Specific energy differences

To evaluate the impact of the variable thermal conductivity $\lambda(T, p_v)$ and of the solar radiation on the specific energy transferred through the opaque component with five different orientations, differences between nominal and actual annual specific energy were calculated. In particular, a distinction between differences of positive transferred energy, towards the external, and negative, towards the internal, was done. Figure 5 and 6 show the increase of positive and negative thermal losses for each location, respectively. Horizontal (roof) and North orientation were chosen for the same reason discussed above. As regards positive thermal losses, it can be noticed that the adoption of a variable thermal conductivity leads to an increase of the energy loss towards the external all over the peninsula: slightly higher losses occur more frequently in the northern than in the southern regions because of the higher temperature difference across the component and, thus, a higher heat flux towards the outside. Indeed, such locations are characterised by a lower annual average external temperature. However, since the solar radiation is less in winter (when larger thermal losses occur) and sol-air temperatures differ just by few degrees one from each other, differences among locations and orientations are not marked. The maximum value was obtained for the North-oriented wall in Rovigo (i.e., 518.1 Wh m^{-2}) and the minimum one for the West-oriented wall in Livorno (i.e., 81.6 Wh m^{-2}).

As regards the negative thermal losses ("thermal gains"), the variable thermal conductivity causes their increase as before. Whereas the thermal losses among orientations are similar, for the negative thermal losses, differences between vertical and horizontal surfaces can be clearly noticed (figure 6). In particular, in case of horizontal surfaces, the maximum negative thermal loss is 675.5 Wh m^{-2} for Reggio Calabria and the minimum one, equal to 205.3 Wh m^{-2}, is found for Feltre, Veneto. The minimum increase for the northern wall is just 19.5 Wh m^{-2} for Forlì.

Table 2 shows the main statistics for the increase of positive and negative thermal losses for North and horizontal orientations.
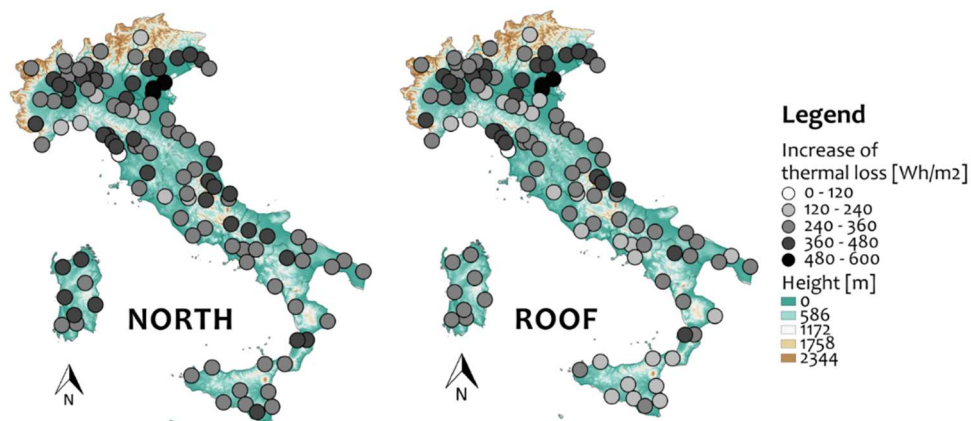
Figure 5. Increase of annual specific thermal losses (positive) calculated with the variable thermal conductivity with respect to the nominal one for northern and horizontal (roof) orientations (Wh m^{-2}).

Figure 6. Increase of annual specific thermal losses (negative) calculated with the variable thermal conductivity with respect to the nominal one for northern and horizontal (roof) orientations (Wh m^{-2}).
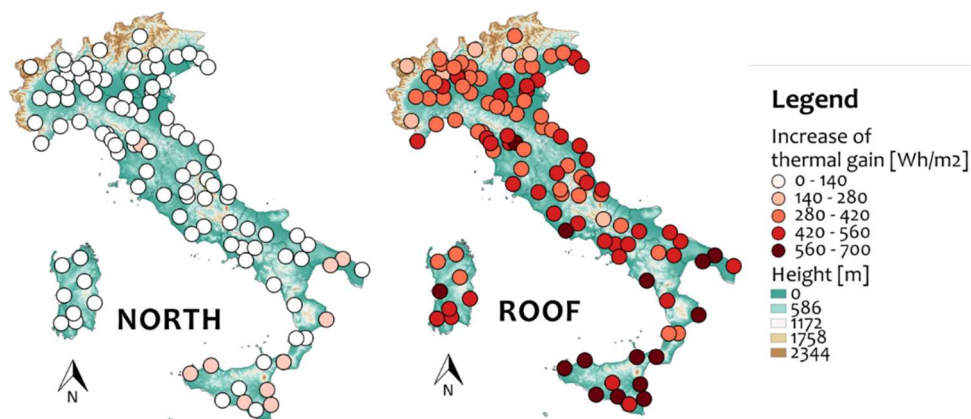
Table 2. Statistics related to the increase of positive and negative thermal losses for north and horizontal orientation (Wh m^{-2}).

	Positive thermal losses		Negative thermal losses	
	North	Horizontal	North	Horizontal
Average (Wh m^{-2})	335.0	306.3	84.9	427.6
Median (Wh m^{-2})	322.7	289.8	78.5	416.6
1st quartile (Wh m^{-2})	278.8	245.5	57.3	343.1
3rd quartile (Wh m^{-2})	394.3	365.2	104.7	503.7
Minimum (Wh m^{-2})	109.5	84.63	19.47	205.3
Maximum (Wh m^{-2})	510.1	518.1	204.4	675.5

4. Conclusions

Thermal conductivity of spruce XLAM can vary significantly from its nominal value if the material is subjected to temperature and moisture conditions deviating from the reference ones. This can lead to uncertainties in the calculated heat transfer and in the energy performance of timber components computed by building simulation codes (e.g., EnergyPlus and TRNSYS) that still adopt constant material thermal properties. To understand the impact of both variable thermal conductivity and the external solar radiation on the heat transfer across such components, at first, an experimental investigation was carried out on spruce specimens, where thermal conductivity was measured at different temperatures and moisture contents. Temperature was varied from 10 to 50 °C and three

different moisture contents (3.5, 6.3 and 13.2 % on a dry basis) were considered and obtained by means of a climatic chamber. Experimental results aimed at obtaining a linear function of the thermal conductivity versus temperature and water vapour partial pressure to be implemented in a 1D finite difference dynamic heat and mass transfer model. The model was calibrated and validated against experimental data. Simulations were run for five 30 cm-thick opaque components, four assumed as vertical walls (South-, East-, North- and West-oriented) and one as a horizontal roof, and for 110 Italian locations. The effect of the solar radiation was accounted with the sol-air temperature.

By comparing simulations run with nominal and variable thermal conductivity, the main results obtained are:

1. The adoption of a variable thermal conductivity leads to an increase of the specific heat flux across XLAM components for any orientation along the Italian peninsula. However, its effect is moderate since the average percentage deviations range from 1 to 5 % considering all the orientations.

2. Among different orientations, the roof has the maximum percentage deviation because of the higher solar radiation on horizontal surfaces, especially in summer. This leads to higher deviations from the nominal heat fluxes and thus, to a higher global deviation.

3. About the increase of thermal losses towards the external, northern regions, in particular the Venetian Plain, are characterised by higher values. This is due to the higher outside relative humidity and lower temperatures. In particular, northern walls are characterised by higher losses since they have no direct radiation. However, differences among orientations are not extremely marked since in winter period, when larger thermal losses occur, solar radiation is lower than in the summer period and it has less effect.

4. Comparing positive thermal losses - towards the external - with either air or sol-air temperature, a slight increase of thermal losses is registered all over the peninsula. Indeed, with the sol-air temperature, the maximum loss is about 518 Wh m^{-2}, while in the other case it is 451 Wh m^{-2}. This is due to the lower peaks of sol-air temperature during the night-time compared to air temperature because of the infrared losses towards the sky vault.

5. About negative thermal losses ("thermal gains"), the variable thermal conductivity leads to an increase of them as for the positive case. In particular, the effect is higher in southern regions and for horizontal orientations (up to 675.5 Wh m^{-2}) because of the location and of the sun path. Higher solar radiation values increase the external surface temperature, increasing the temperature difference across the wall.

6. Considering the solar radiation, thermal gains are three times higher than the case without (i.e., 675.5 Wh m^{-2} vs. 244 Wh m^{-2}). For this reason, the variable thermal conductivity together with the solar radiation influence more thermal gains (in other words the cooling), rather than thermal losses (or heating load).

Further developments of the model will overcome current limitations, including also of the phase change inside the component. This will affect both heat transfer, with latent heat, and mass transfer.

Acknowledgments

5. References

[1]   Suleiman B M, Larfeldt J, Leckner B and Gustavsson M 1999 Influence of temperature and moisture content on the thermal conductivity of wood-based fibreboards *J. Wood Sci. Technol.* **33(6)** 465 −73

[2]   Benichou N, Sultan A M, MacCallum C and Hum J 2001 Thermal properties of wood, gypsum and insulation at elevated temperatures. Internal Report (National Research Council Canada. Institute for Research in Construction); no. IRC-IR-710

[3]   Tafelmeier, S., Longo, G. A., and Gasparella, A, 2016, Energy and Economic Performance Analysis of Heat Recovery Devices Under Different Climate Conditions, International High Performance Buildings Conference, Paper 196, http://docs.lib.purdue.edu/ihpbc/196.

[4]   European committee for Standardization CEN 2007 EN ISO 10456. Building materials and products, Hygrothermal properties, Tabulated design values and procedures for determining declared and design thermal values.

[5]   Budaiwi I and Abdou A 2013 The impact of thermal conductivity change of moist fibrous insulation on energy performance of buildings under hot-humid conditions *J. Energ. Buildings* **41(12)** 1360–67

[6]   Zhao D, Qian X, Gu X, Jajja S A and Yang R n.d. Measurement techniques for thermal conductivity and interfacial thermal conductance of bulk and thin film materials. Retrieved from https://arxiv.org/ftp/arxiv/papers/1605/1605.08469.pdf.

[7]   Engelund Thybring E, Kymäläinen M and Rautkari L 2018 Experimental techniques for characterising water in wood covering the range from dry to fully water-saturated *J. Wood Sci. Technol.* **52** 297–329

[8]   Abdou A A and Budaiwi I M 2004 Comparison of thermal conductivity measurements of building insulation materials under various operating temperatures *J. Bldg. Phys* **29(2)** 171–84

[9]   Jerman M and Černý R 2012 Effect of moisture content on heat and moisture transport and storage properties of thermal insulation materials. *J. Energ. Buildings* **53** 39–46

[10]   Karamanos A, Hadiarakou S and Papadopoulos A M 2008 The impact of temperature and moisture on the thermal performance of stone wool. *J. Energ. Buildings* **40(8)** 1402–11

[11]   CEN 2013 EN ISO 12571. Hygrothermal performance of building materials and products-Determination of hygroscopic sorption properties

[12]   CEN 2000 EN ISO 12570. Hygrothermal performance of building materials and products-Determination of the moisture content by drying at elevated temperature

[13]   Ferroukhi M Y, Belarbi R, Limam K and Bosschaerts W 2017. Experimental validation of a HAM-BES co-simulation approach. *J. Energy procedia* **139** 517–23

[14]   Fitzpatrick J J, O'Sullivan C, Boylan H, Cribben O, Costello D and Cronin K 2013. Moisture sorption isotherm study of Sitka spruce, larch, willow and miscanthus chips and stems. *J. Biosyst. Eng.* **115** 474–481

[15]   CEN 2011 UNI 10375. Metodo di calcolo della temperatura interna estiva degli ambienti.